



## Article

# Advanced Methodology for the Optimal Sizing of the Energy Storage System in a Hybrid Electric Refuse Collector Vehicle Using Real Routes

Ernest Cortez , Manuel Moreno-Eguilaz  and Francisco Soriano

Department of Electronic Engineering MCIA UPC-BarcelonaTech, 08222 Terrassa, Spain; manuel.moreno.eguilaz@upc.edu (M.M.-E.); fsoriano@rosroca.com (F.S.)

\* Correspondence: italovich@gmail.com; Tel.: +34-93-401-1098

Received: 20 September 2018; Accepted: 20 November 2018; Published: 24 November 2018



**Abstract:** This paper presents a new methodology for optimal sizing of the energy storage system (ESS), with the aim of being used in the design process of a hybrid electric (HE) refuse collector vehicle (RCV). This methodology has, as the main element, to model a multi-objective optimisation problem that considers the specific energy of a basic cell of lithium polymer (*Li-Po*) battery and the cost of manufacture. Furthermore, optimal space solutions are determined from a multi-objective genetic algorithm that considers linear inequalities and limits in the decision variables. Subsequently, it is proposed to employ optimal space solutions for sizing the energy storage system, based on the energy required by the drive cycle of a conventional refuse collector vehicle. In addition, it is proposed to discard elements of optimal space solutions for sizing the energy storage system so as to achieve the highest fuel economy in the hybrid electric refuse collector vehicle design phase.

**Keywords:** energy storage; fuel economy; genetic algorithms; optimisation

## 1. Introduction

In cities with high density of population, refuse collector vehicles (RCVs) are of vital importance due to the need to maintain a healthy city. However, the overuse of these trucks leads to a negative impact on the environment because high quantities of fuel are required and contribute to the pollution, aggravated by the automotive industry [1,2].

Accordingly, hybrid electric vehicles (HEVs) and electric vehicles (EVs) offer a solution for the environmental trade-off in terms of pollution problems. However, although HEVs and EVs have great advantages, the HEV is a mature technology in comparison to EV [3,4].

In addition, the HEVs are more feasible for RCV because a larger autonomy is required. Among the HEVs, the RCV is a specific application where the total weight variation, repetitive and aggressive drive cycles are important parameters for its design due to the fact that, although HEVs can cover large distances, a high fuel consumption is required [5]. Then, taking the last consideration on the RCV design, the energy storage system in relation to fuel consumption can be addressed.

Different energy storage elements, such as batteries, supercapacitors or fuel cells, for the energy storage system may be used. For instance, in [6], a hybrid heavy-duty trucks with battery is used, in order to perform a life cycle analysis. In addition, in [7], an energy management strategy for plug-in hybrid electric vehicles based on batteries is proposed.

On the other hand, the supercapacitors may also be used for applications of energy storage. For instance, in [8], a balancing circuit for a hybrid energy storage system with supercapacitor is proposed. In addition, in [9], a current-source converter for a hybrid energy storage system is

performed to interface a supercapacitor (SC) module and a battery stack. Due to the supercapacitor advantages, an increase in the charge/discharge rate and cycling life is achieved [10,11].

Essentially, there are three types of methodologies: sequential, simultaneous and nested, wherein the main purpose is to achieve a *HEV* design optimisation [12]. The structure for each methodology is based on levels such as topology, component sizing and control strategy. Although several layers are defined, the components sizing and the control strategy can fulfil the requirements to achieve the *HEV* optimal design, either for series, parallel or hybrid topology. In addition, taking previous consideration, in several works, the nested methodology is more suitable to obtain a better *HEV* design due to its advantage of low computational times [13,14]. However, for *HEV* design, if the methodologies consider limited parameters to develop a high-performance *HEV*, then an optimal design cannot be achieved.

Accordingly, interest in using more efficient optimisation methods has been increased because the optimal solutions can be delimited through well-defined restrictions. Thereby, the number of evaluations of the objective function decrease and the computational time is reduced [15].

Many optimisation methods have been presented based on a single objective [16–18]. For instance, in [19], the optimal component sizing based on the weight sum method is achieved for a hybrid refuse collector vehicle. In addition, in [20], the energy management of a serial hybrid electric bus with the convex optimisation is performed. Furthermore, in [21], the component sizing of a parallel hybrid electric powertrain by the genetic algorithm is proposed. In addition, the multi-objective optimisation has been presented, wherein the multi-objective optimisation methods are more robust because the space solutions can be delimited. It should be noted that, in the *HEV* design, multi-objective optimisation is required due to the nature of the system, i.e., energy storage system and control strategy.

In accordance with the above, the sizing procedure is considered as a multi-objective problem in [22,23]. For instance, in [24], the component sizing of hybrid hydraulic powertrain by non-dominated sorting genetic algorithm II is performed. In addition, in [25,26], the optimal powertrain component sizing with a multi-objective genetic algorithm is achieved. Nevertheless, real drive cycles are not considered in the optimal sizing methodologies.

Various studies for the industrial vehicles (such as refuse collector vehicle, heavy duty vehicle) have been developed [27–30]. For instance, in [31], the optimal sizing and control of a hybrid tracked vehicle are performed. In addition, in [32], the optimisation problem for the sizing and control of a heavy-duty vehicle is formulated, the solution through several methods (brute force, DIViding RECTangles (DIRECT), sequential quadratic programming (SQP), genetic algorithms (GA) and particle swarm optimisation (PSO)) is achieved. However, the industry demands new methodologies for optimal powertrain sizing.

In this work, a new methodology is developed for optimal sizing of the energy storage system. The manufacturing cost and the volume of a basic cell of lithium polymer (*Li-Po*) battery are considered in the optimisation problem. A multi-objective genetic algorithm is used, with the purpose of obtaining a space of local optimal solutions. Each item from the optimal set allows for sizing the energy storage system, based on the real drive cycle of a conventional refuse collector vehicle. The validation of the proposed methodology is performed through a quasi-static model of an *HE-RCV*, which considers the real behaviour of a *Li-Po* cell. The fuel consumption is calculated, in order to select the energy storage system with the lowest fuel consumption.

In Section 2, a hybrid electric refuse collector vehicle model is presented, taking into account a control strategy. In Section 3, an electrochemical model for the energy storage system is presented. In Section 4, an optimisation problem for sizing of the energy storage system is described. In Section 5, the validation of the methodology is presented. Finally, Section 6 provides the main conclusions of the paper.

## 2. Hybrid Electric Refuse Collector Vehicle

The powertrain of the proposed *HE-RCV* is of the series type configuration, as shown in Figure 1. It consists of one internal combustion engine, two electrical machines and the energy storage system.

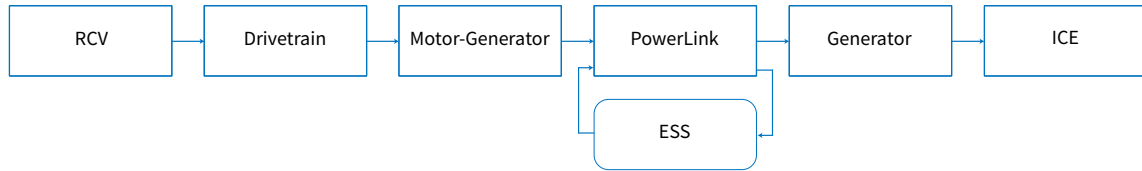


Figure 1. Quasi-static model of an *HE-RCV*.

In this paper, a new methodology is proposed for the optimal sizing of the energy storage system in order to reduce the consumption of the *ICE*, as shown in Figure 2. It is based on the application of a multi-objective genetic algorithm with experimental data of real routes.

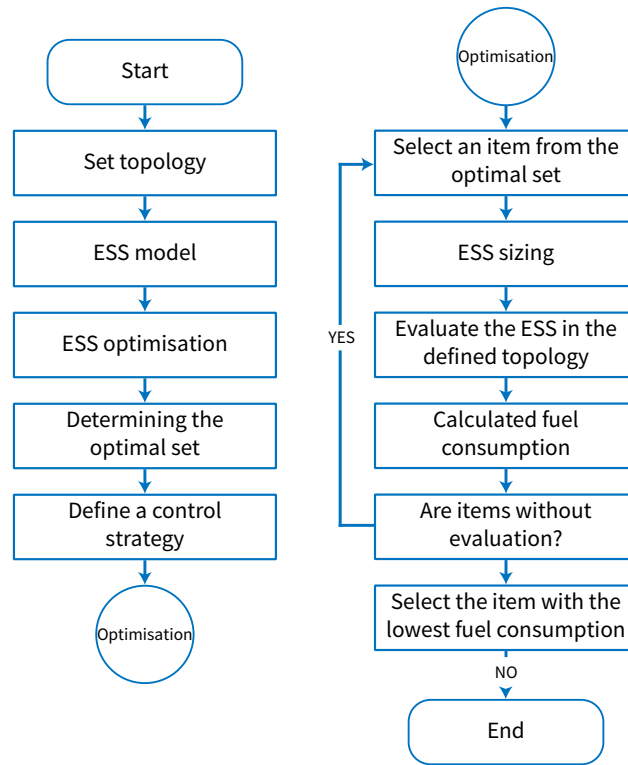


Figure 2. Methodology for optimal sizing of the energy storage system.

To apply this methodology, it is necessary to estimate the fuel consumption of the *HE-RCV* taking into account a control strategy.

The well-known quasi-static model of the *HE-RCV* powertrain includes the longitudinal dynamics [30,33]:

$$m_{RCV} \cdot \frac{d}{dt}v(t) = F_t(t) - (F_a(t) + F_r(t) + F_g(t)), \quad (1)$$

where  $m_{RCV}$  is the mass of the vehicle, taking into account the dynamic load (2) as a characteristic of an RCV,  $F_a$  is the aerodynamic resistance (3),  $F_r$  is the rolling resistance (4), and  $F_g$  is the force caused by gravity during a route on a non-horizontal road (5):

$$m_{RCV} = m_{Vehicle} + m_d(t) + m_{EM} + m_{ESS}, \quad (2)$$

$$F_a = \frac{1}{2} \cdot \rho_a \cdot v^2 \cdot A_f \cdot C_d, \quad (3)$$

$$F_r = m_{RCV} \cdot g \cdot C_r \cdot \cos(\alpha), \quad (4)$$

$$F_g(\alpha) = m_{RCV} \cdot g \cdot \sin(\alpha). \quad (5)$$

Based on the longitudinal dynamics, the power (6) and the energy (7) for the powertrain can be determined:

$$P_{HE-RCV} = F_t(t) \cdot v(t) = m_{RCV} \cdot \frac{d}{dt}v(t) + (F_a(t) + F_r(t) + F_g(t)) \cdot v(t), \quad (6)$$

$$E_{HE-RCV} = \int_0^t P_{HE-RCV} \cdot dt. \quad (7)$$

The transmission plays an important role in the powertrain because there is a linear relationship between torque ( $\tau_{in}$ ) and angular speed ( $\omega_{in}$ ):

$$P_{out} = \frac{\tau_{in} \cdot \omega_{in}}{\gamma}. \quad (8)$$

In order to simplify the estimation of the ICE consumption, the efficiency of the electrical machines is considered constant:

$$P_{out} = \eta_{EM} \cdot P_{in}. \quad (9)$$

The weight of the electrical machines is approximated with a linear dependency with the input power:

$$m_{ME} = 1.685 \cdot P_{in}. \quad (10)$$

The minimum SOC of 20% and a maximum of 100% for the energy storage system is considered [34,35], in order to formulate a rule-based control strategy (11):

$$P_{source} = \begin{cases} ESS, & \text{if } (P_{in} \leq P_{ESS}) \text{ or } (P_{body} \leq P_{ESS}), \\ ICE, & \text{if } (P_{in} > P_{ESS}) \text{ or } (P_{body} > P_{ESS}). \end{cases} \quad (11)$$

In order to protect the ESS front aggressive energy demands, the following condition is imposed:

$$\frac{P_{in}}{V_{ESS} \cdot C_{nom}} \leq C_{discharge}, \quad (12)$$

where  $C_{nom}$  is the rated capacity and  $C_{discharge}$  is the maximum discharge rate.

### 3. Energy Storage System

Although a generic ESS [36–38] may include several elements, such as batteries, supercapacitors [39,40], fuel cells [41], etc., in this paper, only an ESS based on batteries is considered due to its specific energy, energy density and discharge rate.

Several models have been proposed with the intention of reproducing the real electrical behaviour of a battery-based ESS [42]. The proposed ESS is composed of a number of cells connected in series and parallel, in order to provide the required voltage and current. Each cell may be approximated with a first order electrical model, as shown in Figure 3 [43–45].

$V_L$  is the output voltage of the cell:

$$V_L = V_{OC} - R_0 I_L - \int \left( \frac{I_L}{C_1} - \frac{V_{R_1 C_1}}{R_1 C_1} \right) dt, \quad (13)$$

where  $V_{OC}$  is the open circuit voltage of the cell. This voltage may be estimated by using the state of charge (SOC) of the cell:

$$SOC = 100 - \frac{1}{3600 \cdot C} \int I_L(t) dt. \quad (14)$$

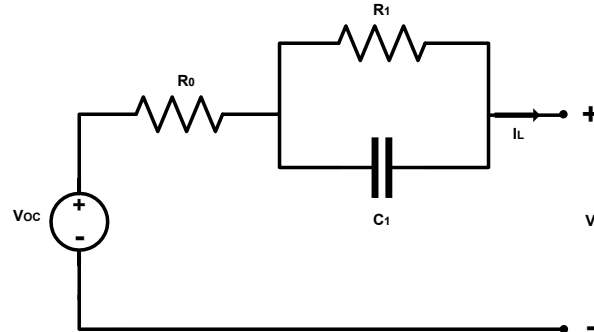


Figure 3. Electrochemical cell model.

The behaviour of the cell can be estimated by experimental measuring of the SOC based on 1C discharge rate beginning at 100 % of SOC. A 1C rate means that the discharge current will discharge the entire battery in one hour. As shown in Figure 4,  $V_L$  is the voltage of the cell when the load is connected with the constant current  $I_L$  and  $V'_L$  is the voltage when the load is disconnected.

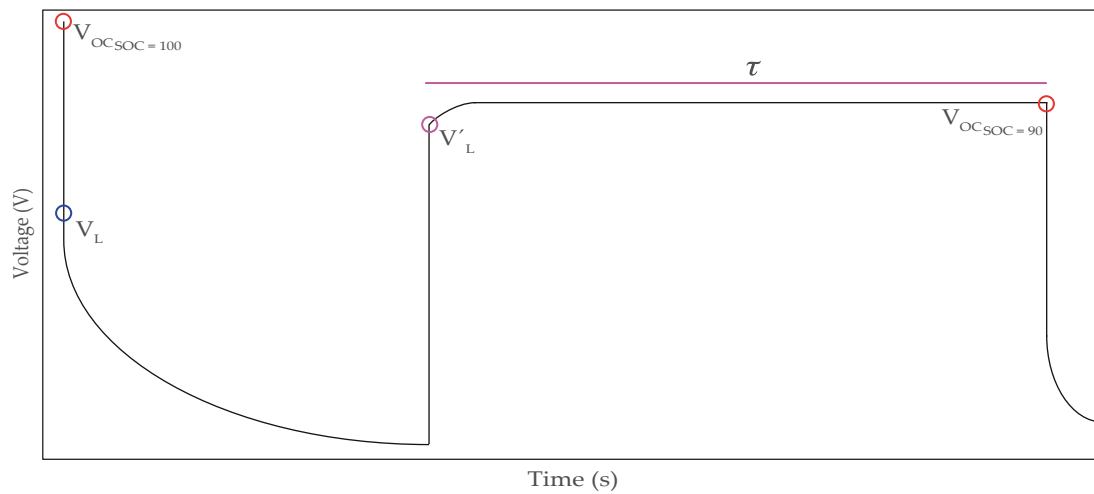


Figure 4. Experimental current discharge in a cell.

It is possible to estimate the value of  $R_0$  (15),  $R_1$  (16) and  $C_1$  (17) for the considered model of the cell (Figure 3) [42,46]:

$$R_0 = \frac{V_{OC} - V_L}{I_L}, SOC = 100, 90, \dots, \quad (15)$$

$$R_1 = \frac{V_{OC} - V'_L}{I_L}, SOC = 100, 90, \dots, \quad (16)$$

$$C_1 = \frac{\tau_{SOC-V'_L}}{R_1}, SOC = 100, 90, \dots \quad (17)$$

Once a cell is experimentally characterised, the parameters of the electric model of the ESS considering  $N_s$  in series are:

$$\begin{aligned}
 V_{OC} &= N_s \cdot V_{OC_{cell}}, \\
 R_1 &= N_s \cdot R_{1_{cell}}, \\
 C_1 &= \frac{1}{N_s} \cdot C_{1_{cell}}.
 \end{aligned}
 \tag{18}$$

#### 4. Optimal Sizing of the ESS

In the design of an *HE-RCV*, one of the most important points is the cost. However, other magnitudes, such as weight, volume, autonomy and efficiency, may be taken into account in order to design a more efficient vehicle. In this work, reduction of cost and volume of the *ESS* are considered in the design of the powertrain.

For these objectives, it is possible to formulate a nonlinear multi-objective optimisation problem under several restrictions, which allows for finding optimal space solutions with a trade-off between the objectives (19):

$$\begin{aligned}
 \min F(x) &= (f_1(x), f_1(x), \dots, f_n(x)), \\
 \text{s.t.} \quad & \\
 g_i &\leq 0, \quad i = 1, \dots, m, \\
 h_i &= 0, \quad i = 1, \dots, m.
 \end{aligned}
 \tag{19}$$

Since it is not possible to correlate the manufacturing cost and the volume of a cell, in this work, it is proposed to use the maximisation of the energy density as an objective in the optimisation problem. Given this cost and density, a continuous nonlinear multi-objective optimisation problem with several constraints is defined:

$$\begin{aligned}
 F(x) &= \begin{cases} \min & \text{cost}(eD), \\ \max & eD(C_{nom}, V_{nom}, L), \end{cases} \\
 \text{s.t.} \quad & \\
 lb_{cost} &\leq \text{cost} \leq ub_{cost}, \\
 lb_{eD} &\leq eD \leq ub_{eD}, \\
 lb_{C_{nom}} &\leq C_{nom} \leq ub_{C_{nom}}, \\
 lb_L &\leq L \leq ub_L,
 \end{aligned}
 \tag{20}$$

where the energy density is computed as:

$$eD = \frac{C_{nom} \cdot V_{nom}}{L}, \tag{21}$$

where  $C_{nom}$  is the rate capacity,  $V_{nom}$  is the rate voltage and  $L$  the volume in a cell.

A multi-objective genetic algorithm is used, as shown in Figure 5, with the purpose to find a finite space of local optimal solutions ( $S$ ) in a limited interval of time. Each element in the optimal solution space defines the characteristics of a cell (22), taking into account the constraints (18):

$$\begin{aligned}
 \{C_{nom}, V_{nom}, L\} &= S(\text{cost}_i, eD_i), i = 1, 2, \dots, n \\
 C_{nom} &\in [lb_{C_{nom}}, ub_{C_{nom}}] \\
 L &\in [lb_L, ub_L].
 \end{aligned}
 \tag{22}$$

Considering the present Li-Po battery technology, the parameters for the multi-objective genetic algorithm are displayed in Table 1.

The number of cells is determined by each element of the optimal solution space:

$$N_s = \frac{C_{ESS}}{C_{nom} \cdot V_{nom}}, \quad (23)$$

where  $C_{ESS}$  (24) is the energy consumed by the powertrain taking into account a real drive cycle:

$$C_{ESS} = \lambda \cdot E_{HE-RCV}. \quad (24)$$

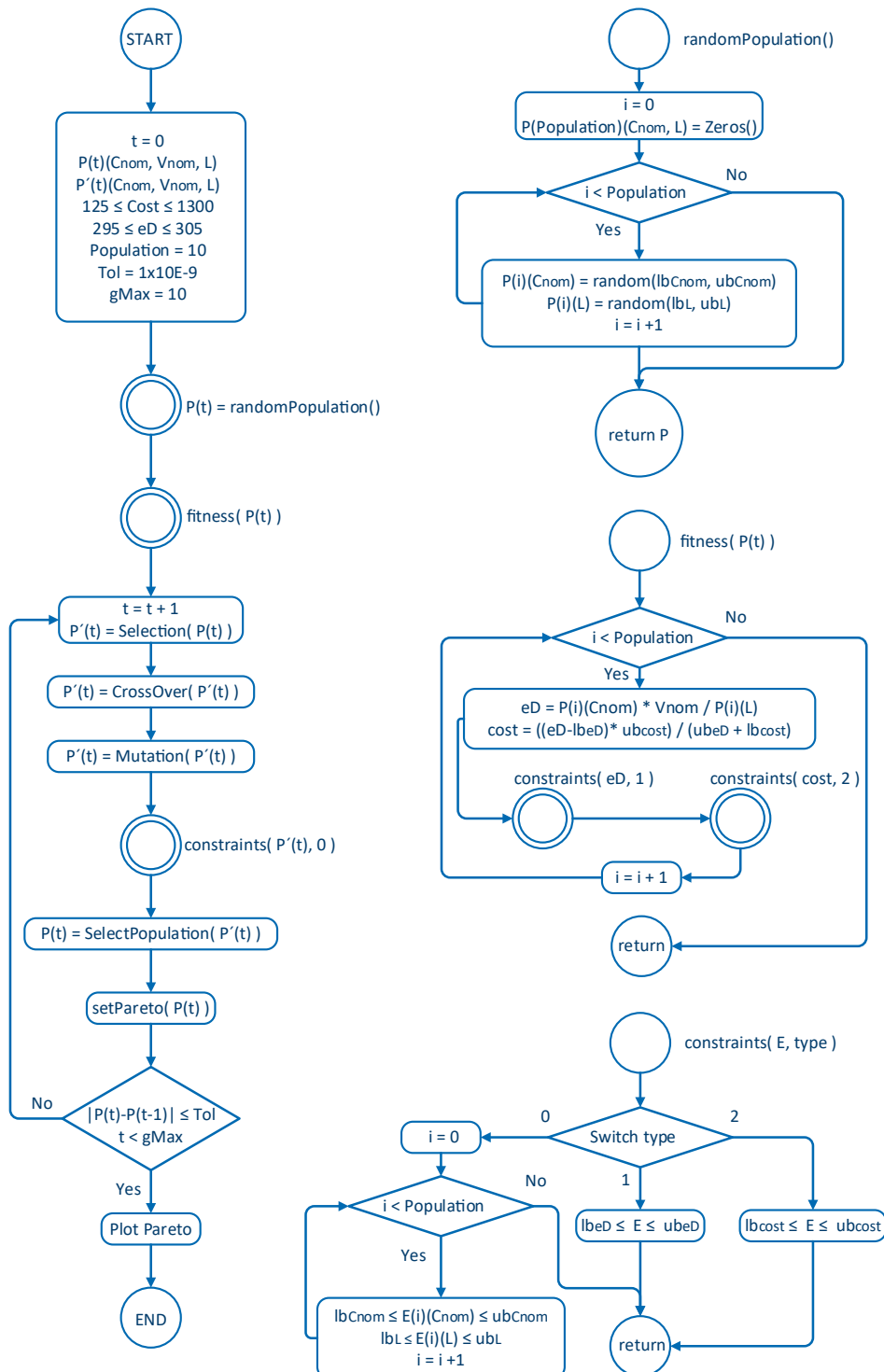


Figure 5. Multi-objective genetic algorithm to achieve a space of local optimal solutions.

The ESS model is defined by (18) using  $N_s$  cells in series.

Then, the final characteristic of ESS is determined through the optimal solution space, taking into account the minimal consumption of the ICE:

$$ICE_{consumption} = \int \frac{\tau_{in} \cdot \omega_{in}}{LHV}, \quad (25)$$

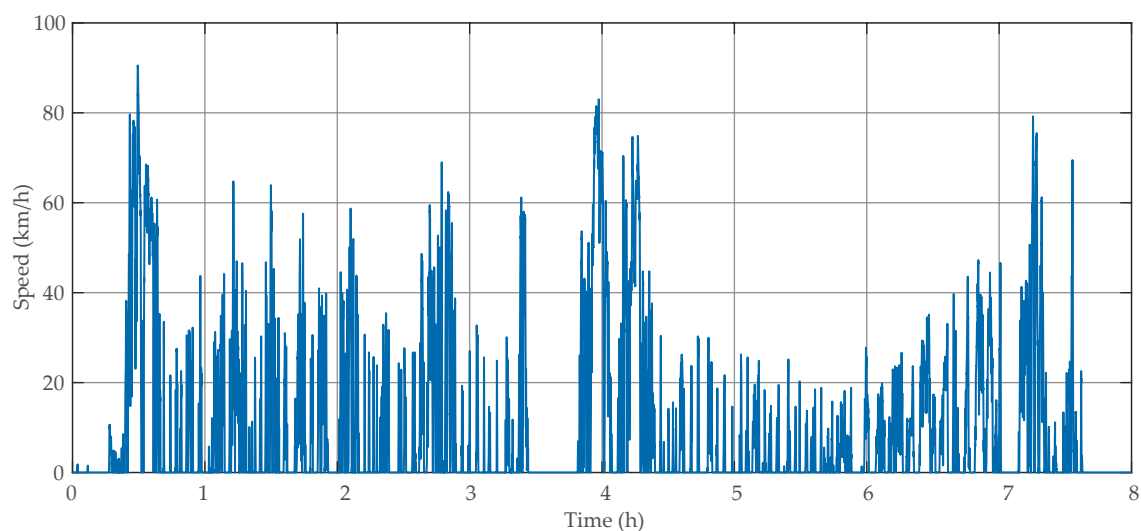
where  $LHV$  is the lower heating value of the fuel.

**Table 1.** Multi-objective genetic algorithm parameters.

Parameters	Value
Manufacturing cost	125–1300 US/kWh
Energy density (eD)	295–305 Wh/L
Objectives	2 ( $Cost$ , $dE$ )
Variables	3 ( $C_{nom}$ , $V_{nom}$ , $L$ )
Population	10
Crossover	0.8
Tolerance	$1 \times 10^{-9}$

## 5. Validation

To validate the proposed methodology, in this work, a real drive cycle from an RCV Iveco Stralis GNC 270 (The vehicle is driven from Tarrega to La Faneca, both in the NE of Spain) is used, as shown in Figure 6. To obtain a real drive cycle, a datalogger CANalyzer CANCase XL (Vector Informatik GmbH, Stuttgart, Germany) with two CAN ports (SN 007130-011289) is used, allowing the storage of torque and rpms of the ICE. These parameters are obtained from the ECM, through the communication bus (CAN J1939) of an RCV during an 8-hour workday. The parameters of this RCV are displayed in Table 2. Based on the maximum collection weight, a dynamic weight profile is proposed, as shown in Figure 7, which distributes the maximum weight during traction moments of drive cycle.

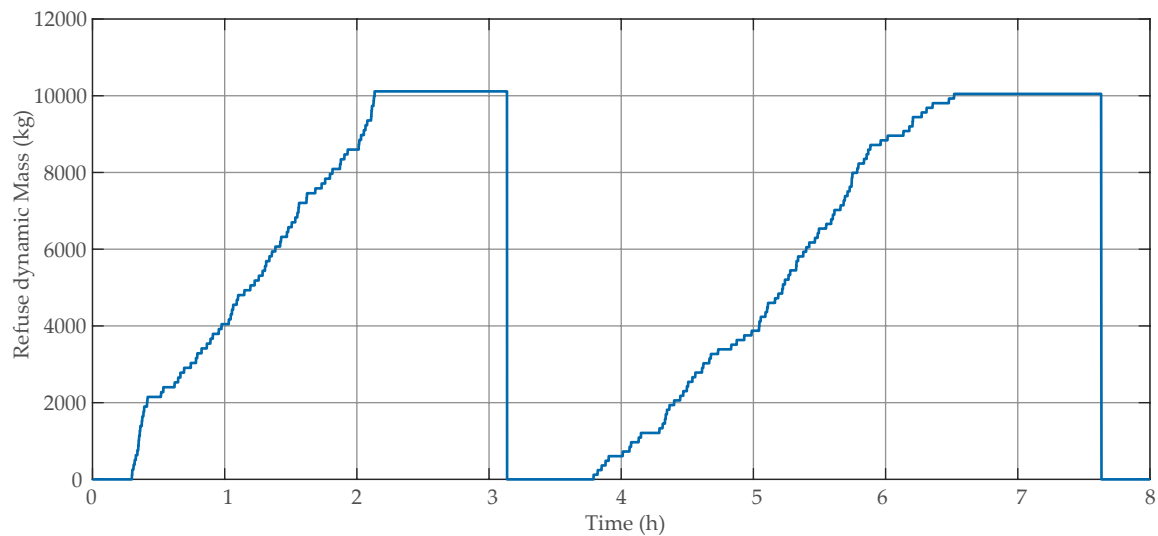


**Figure 6.** Real RCV drive cycle.

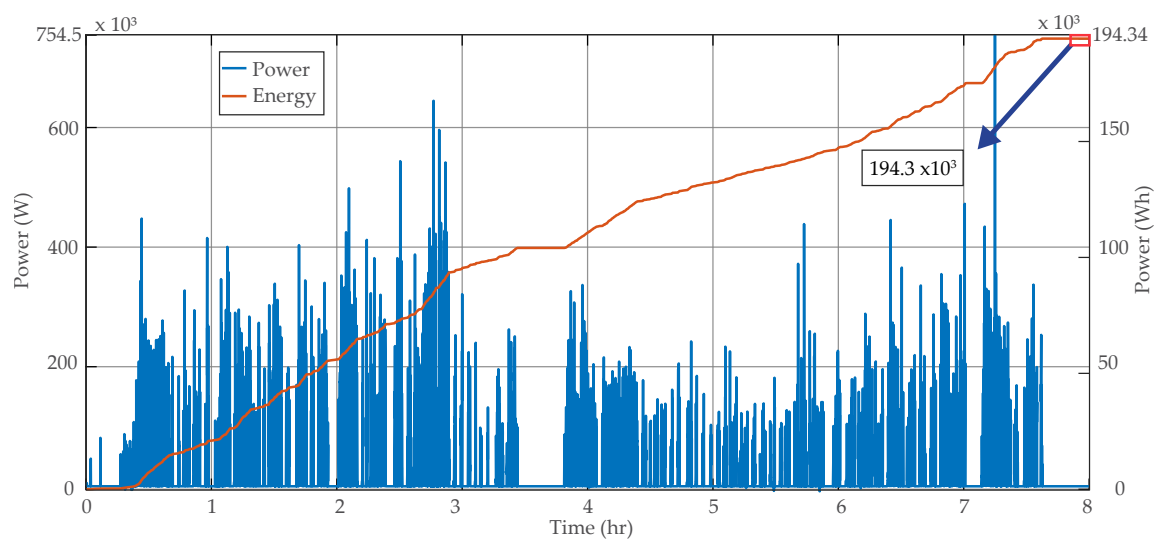


**Table 2.** RCV Characteristics.

Combustion engine	200 kW
Gears	6
Gear ratios ( $\gamma$ )	1 (4.59), 2 (2.25), 3 (1.54) 4 (1.000), 5 (0.75), 6 (0.65)
Weight ( $m_{vehicle}$ )	
(Empty/Full loaded)	15,000/25,000 kg
Frontal area ( $A_f$ )	7.5 m <sup>2</sup>
Drag coefficient ( $C_d$ )	0.6210
Rolling resistance ( $C_r$ )	0.009
Tire (Radius)	315/80/R22.5 (0.5455 m)

**Figure 7.** Dynamic weight profile related to the refuse collector process of an RCV.

Using the quasi-static model described in Section 2, the power and the energy of RCV in a real route is determined, as shown in Figure 8.

**Figure 8.** Power and energy for an HE-RCV taking into account a real drive cycle.

A Li-Po 3.7 V cell is characterised experimentally in order to set the parameters of the model described in Section 3. The state of charge is determined as shown in Figure 9.

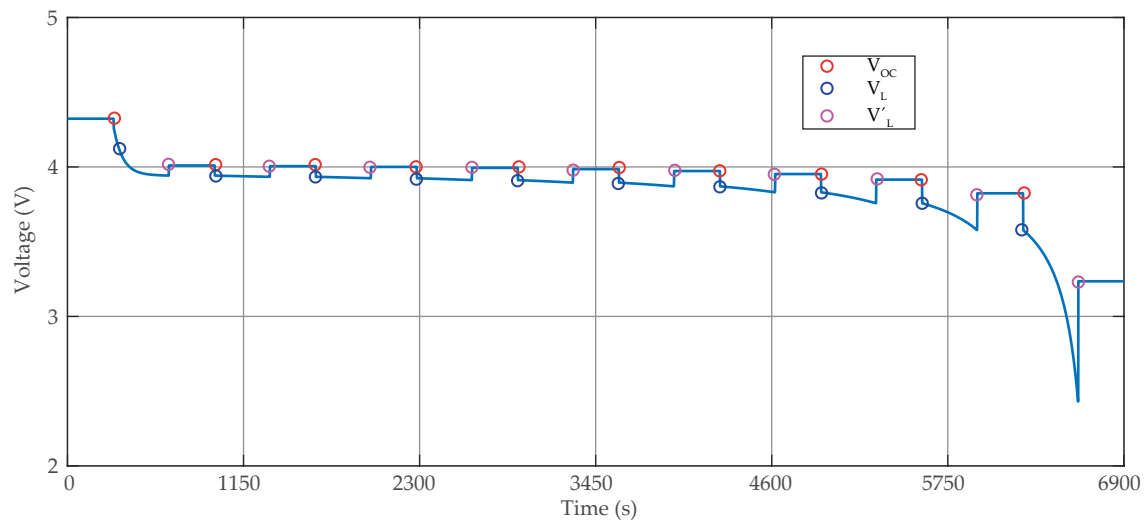


**Figure 9.** SOC with the  $V_{OC}$ ,  $V_L$  and  $V'_L$  identification.

The parameters  $R_0$ ,  $R_1$  and  $C_1$  are determined by using the  $V_{OC}$ ,  $V_L$  and  $V'_L$  for an hour according to 1C discharge rate, as shown in Figures 10–12, respectively.

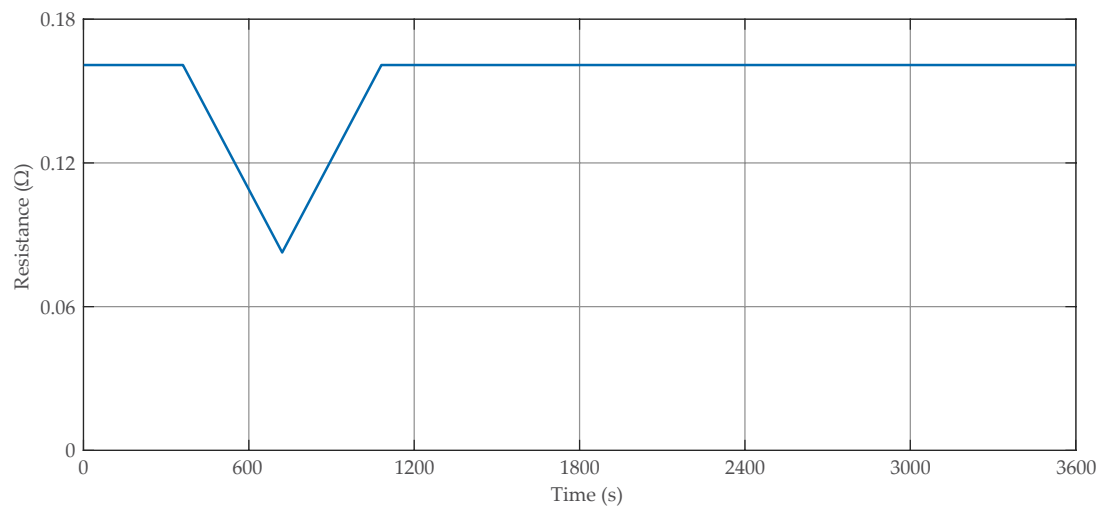


**Figure 10.** Behaviour of the resistance  $R_0$  for a Li-Po cell according to the  $V_{OC}$  and  $V_L$  identification.

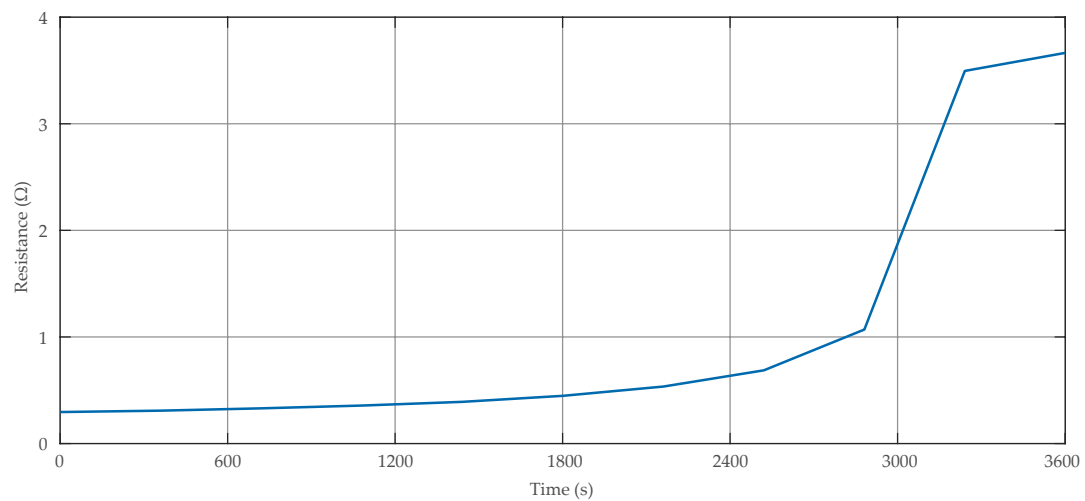


**Figure 11.** Behaviour of the resistance  $R_1$  for a Li-Po cell according to the  $V_{OC}$  and  $V'_L$  identification.

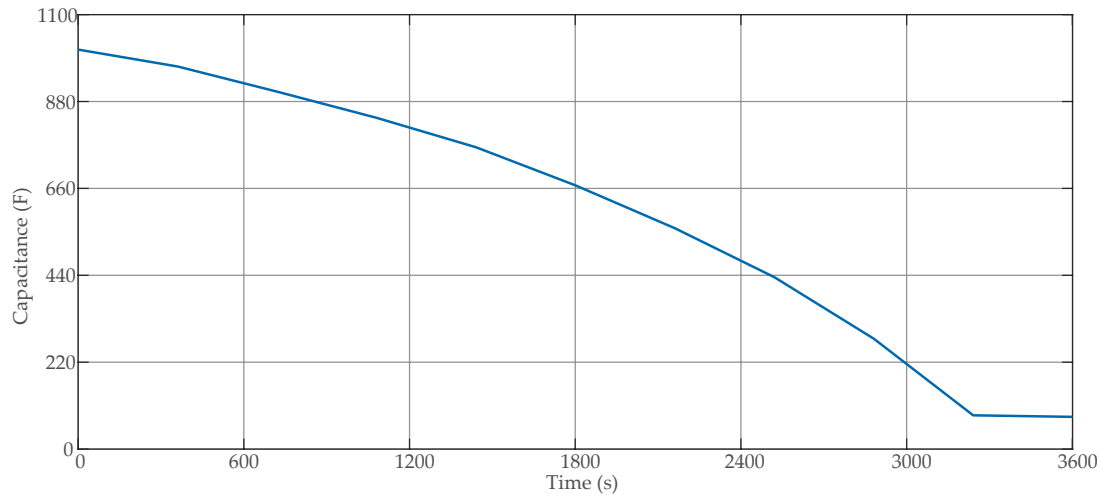


**Figure 12.** Behaviour of the capacitance  $C_1$  for a Li-Po cell according to the  $V_{OC}$ ,  $V_L'$  identification and the  $R_1$  value.

The open circuit voltage  $V_{oc}$  is approximated through the SOC using a lookup table, as shown in Figure 13.

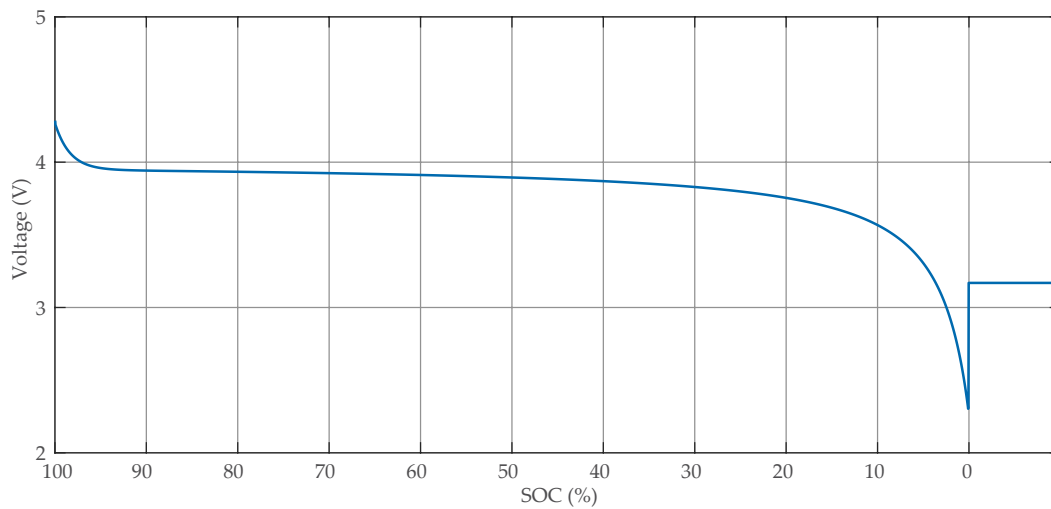


**Figure 13.**  $V_{oc}$  approximation according to the SOC for a Li-Po cell.

Once the cell model has been obtained, the proposed ESS optimisation methodology is applied to find the main parameters (energy density, volume, capacity) of the optimal solutions, taking into account the following constraints:

$$\begin{aligned} lb_{C_{nom}} = 0.2 \text{ A} \leq C_{nom} \leq ub_{C_{nom}} = 20 \text{ A}, \\ lb_L = 0.01 \text{ l} \leq L \leq ub_L = 0.5 \text{ l}. \end{aligned} \quad (26)$$

The space of local optimal solution with the multi-objective genetic algorithm and the particle swarm optimisation (as shown in Figure 14) are compared in Figure 15. Some optimal solution in both optimisation methods are similar; however, based on the optimisation problem, the multi-objective genetic algorithm allows for finding the space of local optimal solutions with a trade-off between the objectives.

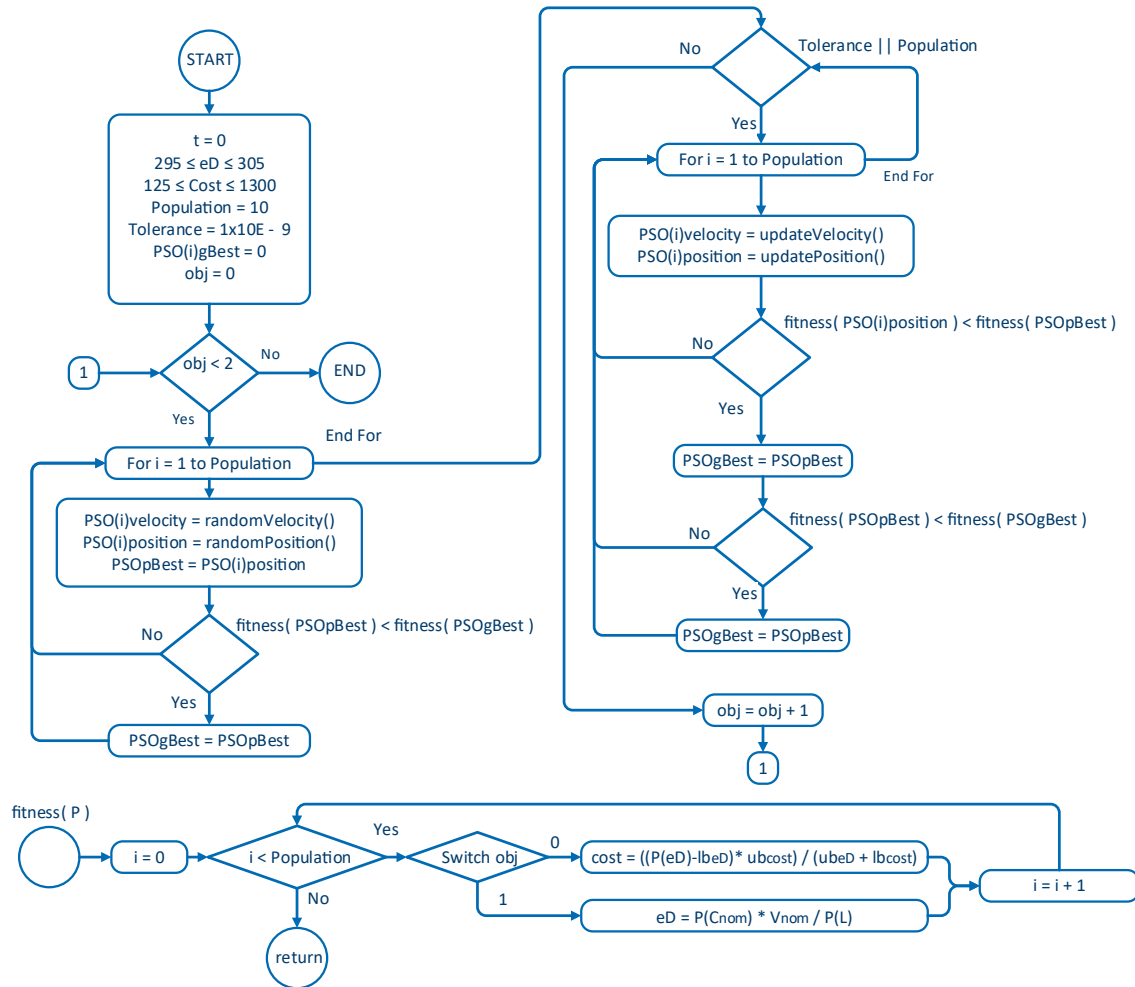


Figure 14. Particle swarm optimisation algorithm.

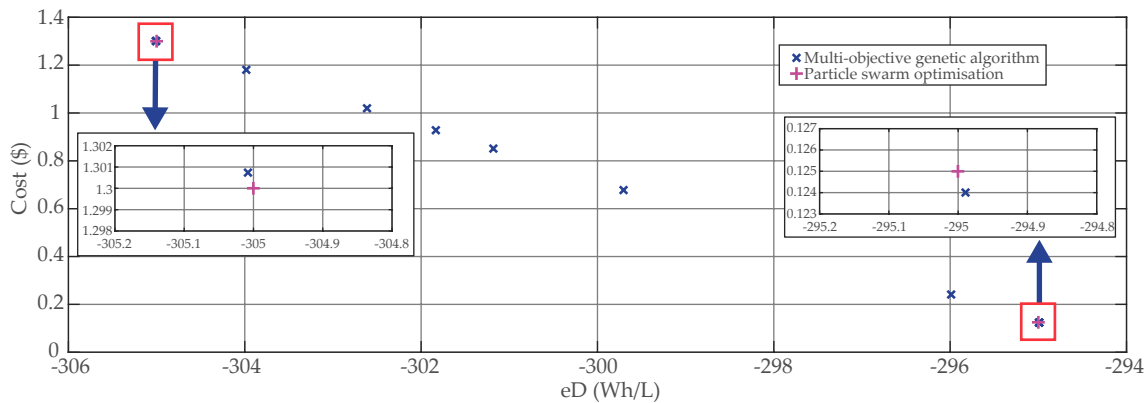


Figure 15. Optimal solution space with the multi-objective genetic algorithm and the particle swarm optimisation for the optimisation problem.

Then, the number of cells in series is calculated by using (24) for each element of the set of optimal space solutions, as shown in Table 3. From the total energy required by the powertrain (Figure 8), in order to validate the present methodology, it is proposed to cover 10% ( $\lambda = 0.1$ ) equivalent to a capacity of  $C_{ESS} = 19.434$  kWh.

A fuel consumption of 30.12 kg was obtained in the conventional vehicle configuration. On the other hand, the calculation was made of the fuel consumption of each element of the set of solutions, as shown in Table 4. The final choice consists of the solution that presents a lower fuel consumption.

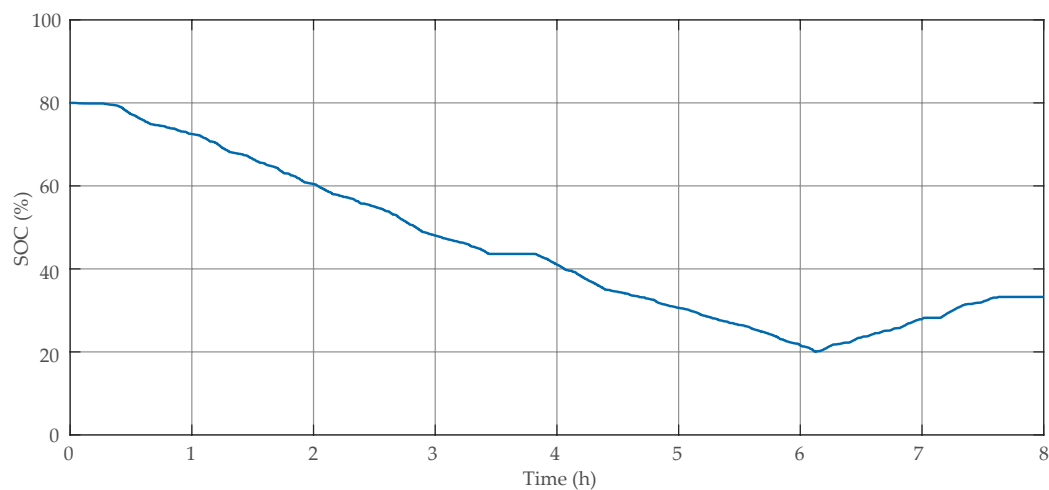
**Table 3.** Optimal solution set.

#	Cost	$eD$ (Wh/L)	$L$ (L)	$C_{nom}$ (Ah)	$N_s$
1	1.300812	−305.006906	0.144788	11.93545	440
2	0.123982	−294.991340	0.115369	9.198045	571
3	0.927891	−301.833114	0.142080	11.59035	453
4	1.300812	−305.006906	0.144788	11.93545	440
5	0.241222	−295.989126	0.115397	9.231446	569
6	0.677771	−299.704430	0.127566	10.33298	508
7	1.180479	−303.982803	0.137194	11.27155	466
8	1.019624	−302.613820	0.142736	11.67404	450
9	0.851227	−301.180651	0.131935	10.73951	489
10	0.123982	−294.991340	0.115369	9.198045	571

**Table 4.** Fuel consumption of *HE-RCV*.

#	$C_{nom}$ (Ah)	$N_s$	Array Capacity (Wh)	Consumption (kg)
1	11.93545	440	19,430.92	19.64
2	9.198045	571	19,432.71	19.61
3	11.59035	453	19,426.60	19.61
4	11.93545	440	19,430.92	19.64
5	9.231446	569	19,434.96	19.03
6	10.33298	508	19,421.88	19.06
7	11.27155	466	19,434.42	20.00
8	11.67404	450	19,437.28	20.00
9	10.73951	489	19,431.00	19.47
10	9.198045	571	19,432.71	19.61

To validate the found optimal solution, the charge/discharge of ESS is shown in Figure 16.

**Figure 16.** ESS state of charge.

## 6. Conclusions

A new methodology is developed for the optimal design of the energy storage system for an *HE-RCV*, which has been validated using real routes from an Iveco Stralis GNC 270 *RCV*.

A model of a nonlinear multi-objective optimisation problem with constraints is achieved, which allows for defining the characteristics of the cell that makes up the *ESS*.

In addition, the cost and volume were set as objectives in the optimisation problem in order to obtain an optimal design of an *ESS*.

To solve the problem, a multi-objective genetic algorithm was used to determine the optimal solutions space and evaluated through an *HE-RCV* with serial topology so as to finally determine the characteristics of the *ESS* that offer the lowest fuel consumption of an *RCV*.

A *Li-Po* cell characterisation is performed through experimental measuring in order to fit the parameters of the cell model.

Furthermore, it was possible to define a control strategy based on rules, which considers the discharge rate of the *ESS*. This allows for improving the design of an *ESS* avoiding the physical damage by a peak discharge.

Finally, the proposed methodology results in an efficient optimal sizing of the *ESS*, achieving a 36.82% reduction in fuel, through an optimal *ESS* that contains an array of 569 cells in series with a capacity of 9.231446 Ah. The *ESS* covers 10% of the energy required by the *RCV* during a real driving cycle. The energy required by the power train is defined as a parameter of the optimal sizing of the *ESS* in the methodology.

The proposed methodology can be used to design an optimal *ESS* considering any percentage of energy required by a hybrid electric vehicle. In addition, this methodology allows for finding the characteristics of an *ESS* with the lowest possible cost and volume.

**Author Contributions:** In this research, E.C. suggested the methodology for the optimal sizing and wrote the manuscript. M.M.-E. suggested the validation of the methodology and revised the manuscript. F.S. made several suggestions to improve the manuscript and made the final revision of the document.

**Funding:** This research received no external funding.

**Acknowledgments:** The authors wish to acknowledge financial support from the Generalitat de Catalunya (GRC MCIA, Grant No. SGR 2014-101).

**Conflicts of Interest:** The authors declare no conflict of interest.

## Abbreviations

The following abbreviations are used in this manuscript:

<i>RCV</i>	Refuse collector vehicle
<i>HEV</i>	Hybrid electric vehicle
<i>HE-RCV</i>	Hybrid electric refuse collector vehicle
<i>EM</i>	Electric machine
<i>ICE</i>	Internal combustion engine
<i>ESS</i>	Energy storage system
<i>ECM</i>	Engine control module
$F_t$	Traction force
$F_a$	Aerodynamic resistance
$F_r$	Rolling resistance
$F_g$	Force caused by gravity
$m_{RCV}$	RCV mass
$m_{vehicle}$	Vehicle mass
$m_d$	Dynamic vehicle mass
$m_{EM}$	EM mass
$m_{ESS}$	ESS mass
$P_{body}$	Body power
$P_{ESS}$	ESS power
$P_{in}$	In power
$P_{out}$	Out power
<i>Li-Po</i>	Lithium polymer battery
$C_{nom}$	Nominal capacity

$C_{ESS}$	ESS capacity
$V_{OC}$	Open-circuit voltage
SOC	State of charge
$eD$	Energy density
$lb$	Lower bound
$ub$	Upper bound

## References

1. Karagulian, F.; Belis, C.A.; Dora, C.F.C.; Pruss-Ustun, A.M.; Bonjour, S.; Adair-Rohani, H.; Amann, M. Contributions to cities' ambient particulate matter (PM): A systematic review of local source contributions at global level. *Atmos. Environ.* **2015**, *120*, 475–483. [\[CrossRef\]](#)
2. Tan, Z. *Air Pollution and Greenhouse Gases: From Basic Concepts to Engineering Applications for Air Emission Control*; Springer: Heidelberg, Germany, 2014; doi:10.1007/978-981-287-212-8.
3. Moghbeli, H.; Niasar, A.H.; Fallahi, N. Fuzzy energy control strategy of through-to-road hybrid electric vehicle. In Proceedings of the 2014 IEEE 23rd International Symposium on Industrial Electronics (ISIE), Istanbul, Turkey, 1–4 June 2014; pp. 1660–1665. [\[CrossRef\]](#)
4. Negarestani, S.; Fotuhi-Firuzabad, M.; Rastegar, M.; Rajabi-Ghahnavieh, A. Optimal Sizing of Storage System in a Fast Charging Station for Plug-in Hybrid Electric Vehicles. *IEEE Trans. Transp. Electr.* **2016**, *2*, 443–453. [\[CrossRef\]](#)
5. Soriano, F.; Moreno-Eguilaz, M.; Alvarez-Florez, J. Drive Cycle Identification and Energy Demand Estimation for Refuse-Collecting Vehicles. *IEEE Trans. Veh. Technol.* **2015**, *64*, 4965–4973. [\[CrossRef\]](#)
6. Rupp, M.; Schulze, S.; Kuperjans, I. Comparative Life Cycle Analysis of Conventional and Hybrid Heavy-Duty Trucks. *World Electr. Veh. J.* **2018**, *9*, 33. [\[CrossRef\]](#)
7. Zeng, Y.; Cai, Y.; Chu, C.; Kou, G.; Gao, W. Integrated Energy and Catalyst Thermal Management for Plug-In Hybrid Electric Vehicles. *Energies* **2018**, *11*, 1761. [\[CrossRef\]](#)
8. Wang, X.; Cheng, K.W.E.; Fong, Y.C. Non-Equal Voltage Cell Balancing for Battery and Super-Capacitor Source Package Management System Using Tapped Inductor Techniques. *Energies* **2018**, *11*, 1037. [\[CrossRef\]](#)
9. Garcia, J.; Garcia, P.; Giulii Capponi, F.; De Donato, G. Analysis, Modeling, and Control of Half-Bridge Current-Source Converter for Energy Management of Supercapacitor Modules in Traction Applications. *Energies* **2018**, *11*, 2239. [\[CrossRef\]](#)
10. Repp, S.; Harputlu, E.; Gurgun, S.; Castellano, M.; Kremer, N.; Pompe, N.; Wörner, J.; Hoffmann, A.; Thomann, R.; Emen, F.M.; et al. Synergetic effects of Fe<sup>3+</sup> doped spinel Li<sub>4</sub>Ti<sub>5</sub>O<sub>12</sub> nanoparticles on reduced graphene oxide for high surface electrode hybrid supercapacitors. *Nanoscale* **2018**, *10*, 1877–1884. [\[CrossRef\]](#) [\[PubMed\]](#)
11. Genc, R.; Alas, M.O.; Harputlu, E.; Repp, S.; Kremer, N.; Castellano, M.; Colak, S.G.; Ocakoglu, K.; Erdem, E. High-Capacitance Hybrid Supercapacitor Based on Multi-Colored Fluorescent Carbon-Dots. *Sci. Rep.* **2017**, *7*, 11222. [\[CrossRef\]](#) [\[PubMed\]](#)
12. Silvaş, E.; Hofman, T.; Steinbuch, M. Review of Optimal Design Strategies for Hybrid Electric Vehicles. *IFAC Proc. Vol.* **2012**, *45*, 57–64. [\[CrossRef\]](#)
13. Lukic, S.M.; Emadi, A. Effects of drivetrain hybridization on fuel economy and dynamic performance of parallel hybrid electric vehicles. *IEEE Trans. Veh. Technol.* **2004**, *53*, 385–389. [\[CrossRef\]](#)
14. Trigui, R.; Vinot, E.; Boujelben, M. Offline optimization for components sizing and analysis of a plug-in hybrid urban microbus. In Proceedings of the 2009 IEEE Vehicle Power and Propulsion Conference, Dearborn, MI, USA, 7–11 September 2009; pp. 382–387. [\[CrossRef\]](#)
15. Silvas, E.; Hofman, T.; Murgovski, N.; Etman, L.F.P.; Steinbuch, M. Review of Optimization Strategies for System-Level Design in Hybrid Electric Vehicles. *IEEE Trans. Veh. Technol.* **2017**, *66*, 57–70. [\[CrossRef\]](#)
16. Souffran, G.; Miegerville, L.; Guerin, P. Simulation of Real-World Vehicle Missions Using a Stochastic Markov Model for Optimal Powertrain Sizing. *IEEE Trans. Veh. Technol.* **2012**, *61*, 3454–3465. [\[CrossRef\]](#)
17. Ravey, A.; Roche, R.; Blunier, B.; Miraoui, A. Combined optimal sizing and energy management of hybrid electric vehicles. In Proceedings of the 2012 IEEE Transportation Electrification Conference and Expo (ITEC), Dearborn, MI, USA, 18–20 June 2012; pp. 1–6. [\[CrossRef\]](#)

18. Pourabdollah, M.; Murgovski, N.; Grauers, A.; Egardt, B. Optimal Sizing of a Parallel PHEV Powertrain. *IEEE Trans. Veh. Technol.* **2013**, *62*, 2469–2480. [[CrossRef](#)]
19. Knoke, T.; Bocker, J. Optimal Power Train Design of a Hybrid Refuse Collector Vehicle. In Proceedings of the 2007 IEEE Vehicle Power and Propulsion Conference, Arlington, TX, USA, 9–12 September 2007; pp. 815–820. [[CrossRef](#)]
20. Elbert, P.; Nüesch, T.; Ritter, A.; Murgovski, N.; Guzzella, L. Engine On/Off Control for the Energy Management of a Serial Hybrid Electric Bus via Convex Optimization. *IEEE Trans. Veh. Technol.* **2014**, *63*, 3549–3559. [[CrossRef](#)]
21. Gao, W.; Porandla, S.K. Design optimization of a parallel hybrid electric powertrain. In Proceedings of the 2005 IEEE Vehicle Power and Propulsion Conference, Chicago, IL, USA, 7–9 September 2005; p. 6. [[CrossRef](#)]
22. Vinot, E.; Reinbold, V.; Trigui, R. Global Optimized Design of an Electric Variable Transmission for HEVs. *IEEE Trans. Veh. Technol.* **2016**, *65*, 6794–6798. [[CrossRef](#)]
23. Vincent, R.; Emmanuel, V.; Lauric, G.; Laurent, G. Optimal sizing of an electrical machine using a magnetic circuit model: application to a hybrid electrical vehicle. *IET Electr. Syst. Transp.* **2016**, *6*, 27–33. [[CrossRef](#)]
24. Moulik, B.; Karbaschian, M.A.; Soffker, D. Size and Parameter Adjustment of a Hybrid Hydraulic Powertrain Using a Global Multi-Objective Optimization Algorithm. In Proceedings of the 2013 IEEE Vehicle Power and Propulsion Conference (VPPC), Beijing, China, 15–18 October 2013; pp. 1–6. [[CrossRef](#)]
25. Desai, C.; Williamson, S.S. Optimal design of a parallel Hybrid Electric Vehicle using multi-objective genetic algorithms. In Proceedings of the 2009 IEEE Vehicle Power and Propulsion Conference, Dearborn, MI, USA, 7–11 September 2009; pp. 871–876. [[CrossRef](#)]
26. Jain, M.; Desai, C.; Kharm, N.; Williamson, S.S. Optimal powertrain component sizing of a fuel cell plug-in hybrid electric vehicle using multi-objective genetic algorithm. In Proceedings of the 2009 35th Annual Conference of IEEE Industrial Electronics, Porto, Portugal, 3–5 November 2009; pp. 3741–3746. [[CrossRef](#)]
27. Serrao, L.; Rizzoni, G. Optimal control of power split for a hybrid electric refuse vehicle. In Proceedings of the 2008 American Control Conference, Seattle, WA, USA, 11–13 June 2008; pp. 4498–4503. [[CrossRef](#)]
28. Ravey, A.; Watrin, N.; Blunier, B.; Miraoui, A. Energy sources sizing for hybrid fuel cell vehicles based on statistical description of driving cycles. In Proceedings of the 2010 IEEE Vehicle Power and Propulsion Conference, Lille, France, 1–3 September 2010; pp. 1–6. [[CrossRef](#)]
29. Soriano, F.; Alvarez-Florez, J.; Moreno-Eguilaz, M. Experimentally Compared Fuel Consumption Modelling of Refuse Collecting Vehicles for Energy Optimization Purposes. *SAE Int. J. Commer. Veh.* **2014**, *7*, 324–336. [[CrossRef](#)]
30. Zhao, D.; Stobart, R.; Dong, G.; Winward, E. Real-Time Energy Management for Diesel Heavy Duty Hybrid Electric Vehicles. *IEEE Trans. Control Syst. Technol.* **2015**, *23*, 829–841. [[CrossRef](#)]
31. Zou, Y.; Sun, F.; Hu, X.; Guzzella, L.; Peng, H. Combined Optimal Sizing and Control for a Hybrid Tracked Vehicle. *Energies* **2012**, *5*, 4697–4710. [[CrossRef](#)]
32. Silvas, E.; Bergshoeff, E.; Hofman, T.; Steinbuch, M. Comparison of Bi-Level Optimization Frameworks for Sizing and Control of a Hybrid Electric Vehicle. In Proceedings of the 2014 IEEE Vehicle Power and Propulsion Conference (VPPC), Coimbra, Portugal, 27–30 October 2014; pp. 1–6. [[CrossRef](#)]
33. Guzzella, L.; Amstutz, A. CAE tools for quasi-static modeling and optimization of hybrid powertrains. *IEEE Trans. Veh. Technol.* **1999**, *48*, 1762–1769. [[CrossRef](#)]
34. Carkhuff, B.G.; Demirev, P.A.; Srinivasan, R. Impedance-Based Battery Management System for Safety Monitoring of Lithium-Ion Batteries. *IEEE Trans. Ind. Electr.* **2018**, *65*, 6497–6504. [[CrossRef](#)]
35. Armstrong, T.; Nork, S. *Maximize the Run Time in Automotive Battery Stacks Even as Cells Age*; Technical report; Analog Devices: Norwood, MA, USA, 2017.
36. Li, Q.; Chen, W.; Li, Y.; Liu, S.; Huang, J. Energy management strategy for fuel cell/battery/ultracapacitor hybrid vehicle based on fuzzy logic. *Int. J. Electr. Power Energy Syst.* **2012**, *43*, 514–525. [[CrossRef](#)]
37. Ostadi, A.; Kazerani, M.; Chen, S.K. Hybrid Energy Storage System (HESS) in vehicular applications: A review on interfacing battery and ultra-capacitor units. In Proceedings of the 2013 IEEE Transportation Electrification Conference and Expo (ITEC), Detroit, MI, USA, 16–19 June 2013; pp. 1–7. [[CrossRef](#)]
38. Chemali, E.; Preindl, M.; Malysz, P.; Emadi, A. Electrochemical and Electrostatic Energy Storage and Management Systems for Electric Drive Vehicles: State-of-the-Art Review and Future Trends. *IEEE J. Emerg. Sel. Top. Power Electr.* **2016**, *4*, 1117–1134. [[CrossRef](#)]



39. Passalacqua, M.; Lanzarotto, D.; Repetto, M.; Marchesoni, M. Advantages of Using Supercapacitors and Silicon Carbide on Hybrid Vehicle Series Architecture. *Energies* **2017**, *10*, [[CrossRef](#)]
40. Wang, Y.; Yang, Z.; Li, F. Optimization of Energy Management Strategy and Sizing in Hybrid Storage System for Tram. *Energies* **2018**, *11*, [[CrossRef](#)]
41. Aschilean, I.; Varlam, M.; Culcer, M.; Iliescu, M.; Raceanu, M.; Enache, A.; Raboaca, M.S.; Rasoi, G.; Filote, C. Hybrid Electric Powertrain with Fuel Cells for a Series Vehicle. *Energies* **2018**, *11*, [[CrossRef](#)]
42. Fotouhi, A.; Auger, D.J.; Propp, K.; Longo, S.; Wild, M. A review on electric vehicle battery modelling: From Lithium-ion toward Lithium–Sulphur. *Renew. Sustain. Energy Rev.* **2016**, *56*, 1008–1021. [[CrossRef](#)]
43. Zhuang, W.; Wang, L.; Yin, Z.; Ye, J.; Wu, H. Optimal energy management strategy design for a diesel parallel hybrid electric vehicle. In Proceedings of the 11th IEEE International Conference on Control & Automation (ICCA), Taichung, Taiwan, 18–20 June 2014; pp. 1050–1055. [[CrossRef](#)]
44. Ostadi, A.; Kazerani, M. A Comparative Analysis of Optimal Sizing of Battery-Only, Ultracapacitor-Only, and Battery; Ultracapacitor Hybrid Energy Storage Systems for a City Bus. *IEEE Trans. Veh. Technol.* **2015**, *64*, 4449–4460. [[CrossRef](#)]
45. Barcellona, S.; Grillo, S.; Piegari, L. A simple battery model for EV range prediction: Theory and experimental validation. In Proceedings of the 2016 International Conference on Electrical Systems for Aircraft, Railway, Ship Propulsion and Road Vehicles & International Transportation Electrification Conference (ESARS-ITEC), Toulouse, France, 2–4 November 2016; pp. 1–7. [[CrossRef](#)]
46. Ceylan, M.; Sarikurt, T.; Balıkcı, A. A novel Lithium-Ion-Polymer battery model for hybrid/electric vehicles. In Proceedings of the 2014 IEEE 23rd International Symposium on Industrial Electronics (ISIE), Istanbul, Turkey, 1–4 June 2014; pp. 366–369. [[CrossRef](#)]



© 2018 by the authors. Licensee MDPI, Basel, Switzerland. This article is an open access article distributed under the terms and conditions of the Creative Commons Attribution (CC BY) license (<http://creativecommons.org/licenses/by/4.0/>).